

Determination of the s-wave Scattering Length of Chromium

P. O. Schmidt, S. Hensler, J. Werner, A. Griesmaier, A. Gorlitz, and T. Pfau
 5. Physikalisches Institut, Universitat Stuttgart, 70550 Stuttgart, Germany

A. Simoni
 Dipartimento di Chimica, Universitat di Perugia, 06123 Perugia, Italy
 (Dated: February 9, 2020)

We have measured the deca-triplet s-wave scattering length of the bosonic chromium isotopes ^{52}Cr and ^{50}Cr . From the time constants for cross-dimensional thermalization in atomic samples we have determined the magnitudes $|a(^{52}\text{Cr})| = (170 \pm 39) a_0$ and $|a(^{50}\text{Cr})| = (40 \pm 15) a_0$, where $a_0 = 0.053 \text{ nm}$. By measuring the thermalization rate of ^{52}Cr over a wide temperature range and comparing the temperature dependence with the effective-range theory and single-channel calculations, we have obtained strong evidence that the sign of $a(^{52}\text{Cr})$ is positive. Rescaling our ^{52}Cr model potential to ^{50}Cr strongly suggests that $a(^{50}\text{Cr})$ is positive, too.

PACS numbers: 34.50.{s, 34.50.P, 03.65.Nk, 32.80.Pj}

With the development of laser cooling and trapping techniques, atomic collisional properties in the ultracold regime have become directly accessible. Today these properties play a crucial role for the realization of Bose-Einstein condensates (BECs) and quantum degenerate samples of fermions by evaporative cooling [1]. In the ultracold regime, elastic collisions between neutral atoms are dominated by s-wave scattering which can be characterized by a single parameter, the s-wave scattering length. Pure and stable BECs could so far only be realized if the scattering length is positive and has a value in the range from 50 to 300 a_0 . Exceptions are ^7Li [2] with a negative scattering length which forms only condensates with limited number and hydrogen [3] with a very small scattering length where condensate fractions of no more than 5% have been reached. In ^{85}Rb [4] and ^{133}Cs [5], Feshbach resonances have been used to tune the scattering length into the right range for achieving BEC. Therefore, a careful measurement of the scattering length is a first requirement before a strategy for the condensation of a new atomic species can be devised.

However, elastic collisions are not only essential for evaporative cooling of an atomic gas but they also determine the interaction in a quantum degenerate gas. The presence of this interaction is also responsible for many of the fascinating features of BECs like superfluid behavior or the existence of phonon-like excitations [1]. In the case of chromium, the magnitude of the scattering length will also determine how significant the effects of the anisotropic dipole-dipole interaction will be [6].

Up to now, only the s-wave scattering lengths for alkali atoms, hydrogen and metastable helium have been measured. The most precise methods are probably photo-association spectroscopy [7, 8] and Raman spectroscopy [9] between vibrational levels of the electronic molecular ground state. Another possibility is Feshbach resonance spectroscopy [10, 11, 12] where the position and magnetic field dependence of several Feshbach resonances is

determined.

For chromium, no molecular spectroscopy data are available for the deca-triplet state which (neglecting the spin-spin interaction) corresponds to the collisional channel for elastic collisions in samples prepared in spin-stretched (i.e. $j_{\text{in}} j = J$) states. Due to the complicated electronic structure with six unpaired outer-shell electrons, accurate ab initio calculations of the molecular potentials are also not available. Fortunately near-threshold collisions are not sensitive to the details of the short-range interaction potential. They are to a large extent determined by the s-wave scattering length and by the long-range dispersion interaction, characterized by the leading van der Waals coefficient C_6 .

In this paper, we report on a measurement of the s-wave scattering length of bosonic chromium atoms, spin polarized in the weak-field seeking $J = m_J = 3$ state, from cross-dimensional relaxation in a magnetic trap. By recording the relaxation of an anisotropic temperature distribution in an atomic cloud towards equilibrium, we obtain a relaxation time constant which is proportional to the effective scattering cross-section through the atomic density. This method has been first used by Monroe et al. [13] for ^{133}Cs and has since been employed to determine the ultra-cold scattering properties of many other alkaline metals. In all of these experiments, only the scattering cross section, i.e. the magnitude of the scattering length could be determined, but not its sign. As shown by Ferrari et al. [14], also the sign of the scattering length can in some instances be determined by a careful measurement of the temperature dependence of the scattering cross section.

We have determined values of $|a(^{52}\text{Cr})| = (170 \pm 39) a_0$ and $|a(^{50}\text{Cr})| = (40 \pm 15) a_0$. A careful analysis of the temperature-dependence of the cross section for ^{52}Cr in a range from 5 to 500 K allowed us to compare the experimental data to the effective-range theory. From this comparison, we have obtained strong evidence that the scat-

tering length of ^{52}Cr is positive. Due to its much lower natural abundance, we could only measure the cross section for ^{50}Cr over a smaller temperature range. Rescaling a ^{52}Cr model potential to ^{50}Cr strongly suggests a positive scattering length also for ^{50}Cr .

The experimental setup is described in detail in [15, 16] and is only outlined here. We prepare magnetically trapped, spin-polarized clouds of chromium atoms by using our CLIP trap loading procedure [15]. After loading, the atoms are Doppler cooled in the magnetic trap [16]. Further cooling is achieved by forced rf-evaporation in a magnetic trap with an offset field of 4 G and trap frequencies of $\omega_r = \omega_x = \omega_y = 2\pi 124\text{ Hz}$ and $\omega_z = 2\pi 72.6\text{ Hz}$, where the temperature can be adjusted by varying the end frequency of the rf ramp. Subsequently, the magnetic offset field is ramped within 25 ms from 4 to 1.75 G which increases ω_r to $2\pi 207\text{ Hz}$. Since the time scale for the modification of the trap is much faster than the mean time between collisions, this creates an anisotropic temperature distribution $T(t)$. To observe rethermalization, absorption images in the trap are taken after variable wait times between 10 ms and 2 s. The radial and axial temperatures can then be inferred from the corresponding sizes of the cloud and the known trap frequencies. The number of atoms and thus the density is calibrated by taking additional absorption images after release of the atoms from the trap.

If no additional heating is present, the anisotropic distribution relaxes to the new steady state temperature $T^f = T_r^f = T_z^f = (2T_r^i + T_z^i)/3$ via elastic collisions. In the real experimental situation, inelastic processes dominated by dipolar relaxation rates cause heating and atom loss, with a significant decrease of the gas density during relaxation. If the typical time scale for atom loss is longer than the relaxation time, the density decrease can be accounted for by employing a time rescaling method [17]. In our relaxation measurements, the lifetime of the atomic sample exceeded the relaxation time constant by at least a factor of 10.

Fig. 1 shows a typical relaxation measurement for a cloud with a mean temperature of $T(t) = (2T_r(t) + T_z(t))/3 = 42\text{ K}$. In the inset, we have plotted the evolution of the mean temperature where the slight increase for long thermalization times can be attributed to dipolar relaxation collisions. An exponential fit to $T(t)$, where t^* is the rescaled time, yields a relaxation time constant τ_{rel} . We have experimentally verified, that the relaxation time constant is inversely proportional to the density of the cloud, thus ruling out anharmonic mixing.

The experimentally observed rethermalization rate is related to the atomic collision rate by $\tau_{\text{coll}} = \tau_{\text{rel}}$, where τ is in general a temperature-dependent proportionality factor. The elastic collision rate τ_{coll} in a non-degenerate ultra-cold gas in thermal equilibrium is given by $\tau_{\text{coll}} = n(t) \langle (v_r) v_r \rangle_{\text{th}}$, where $\langle \dots \rangle_{\text{th}}$ denotes

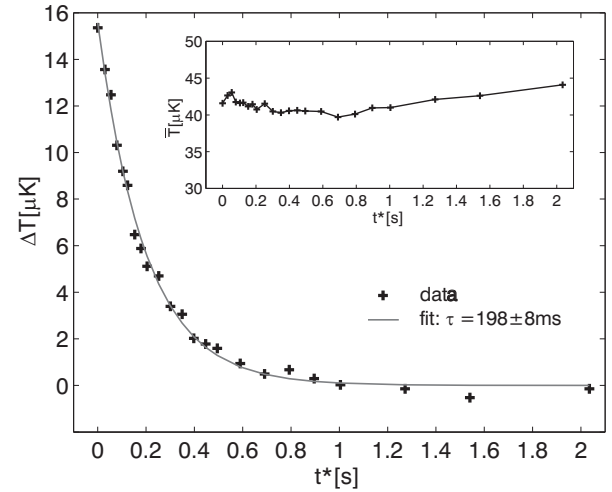


FIG. 1: Thermal relaxation versus rescaled time t^* of a cloud of ^{52}Cr atoms in a magnetic trap. The initial anisotropic temperature distribution is created by a sudden change of the radial trap frequency from $\omega_r = 2\pi 124\text{ Hz}$ to $\omega_r = 2\pi 207\text{ Hz}$. The line is an exponential fit to the data. The inset shows the evolution of the mean temperature of the cloud.

thermal averaging and $n = \frac{R}{n^2(\mathbf{r})dV} = \frac{R}{n(\mathbf{r})dV}$ is the mean density. The proportionality factor can take values from $\tau = 2.65$ for a energy-independent elastic cross section [13, 18, 19] to $\tau = 10.7$ for an energy-dependent cross section in the unitarity limit [18, 19]. A detailed analysis of our experiment shows that the situation is intermediate. Therefore, we use the analytical result [19], Eqs. (72) and (88)

$$\tau_{\text{rel}}(T) = \frac{1}{4} n \langle (v_r) v_r \rangle_{\text{sth}} \quad (1)$$

for the relaxation rate to analyze our data, where $\langle \dots \rangle_{\text{sth}}$ denotes the non-standard thermal average required for relaxation of thermal anisotropies.

In order to obtain the scattering length, we use the effective-range approximation to the collisional cross-section [20],

$$= \frac{8 a^2}{k^2 a^2 + (\frac{1}{2} k^2 r_{\text{eff}} - 1)^2}; \quad (2)$$

where k is the relative wave vector, a the scattering length and r_{eff} the effective range of the potential. The latter can be derived from the scattering length and the C_6 coefficient [21, 22]. For chromium, we obtain from the static polarizability [23] $C_6 = (1050 \pm 200) \text{ a.u.}$, where 1 a.u. = $9.57 \cdot 10^{-80} \text{ J m}^6$. In the temperature range we explore, the non-resonant contribution of higher order partial waves to the elastic cross section can be neglected, since for chromium the threshold temperature for d-waves is on the order of 1.3 mK [24].

The magnitude of the scattering length can be more accurately determined from low temperature measurements

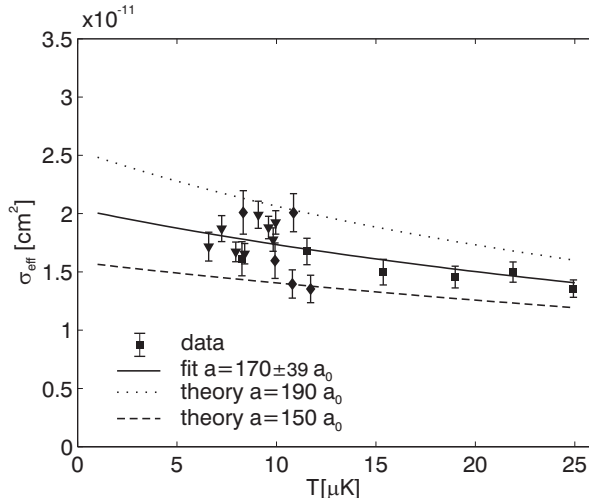


FIG. 2: Temperature dependence of the effective elastic cross section of ^{52}Cr for $T \neq 0$. The full line is a fit to the data yielding $a(^{52}\text{Cr}) = (170 \pm 39) a_0$. The dotted (dashed) line is a theoretical curve derived from Eqs. 1 and 3 for a positive scattering length of $190 a_0$ ($150 a_0$). The error bars are derived from statistical and calibration uncertainties.

of the elastic cross section. In Fig. 2, we have plotted the effective elastic cross section [28]

$$\sigma_e(T) = \frac{2.65 \frac{r_e(T)}{n < v_r >_{th}}}{(3)}$$

for temperatures below 25 K. Here $< v_r >_{th} = \frac{1}{2} 16k_B T = m$ is the relative thermal velocity with k_B the Boltzmann constant and m the chromium mass. The solid curve in Fig. 2 is a fit of Eq. (1) to the data points shown, yielding a scattering length of $a(^{52}\text{Cr}) = (170 \pm 39) a_0$ corresponding, for the nominal C_6 , to an effective range of $r_e = 83 a_0$. The given error combines statistical and systematic uncertainties where the dominant contribution is from a systematic uncertainty of 20% in the determination of the density of the atomic cloud.

The sign of the scattering length can be deduced from a comparison of the measured temperature dependence of the relaxation rate with theoretical models over a sufficiently large temperature range. We have performed relaxation rate measurements for ultra-cold ^{52}Cr covering a temperature range of approximately two orders of magnitude. The result is shown in Fig. 3 where we have plotted the density-normalized relaxation rate Γ_{rel}/\bar{n} versus the mean temperature of the atomic sample. We have plotted Eq. (1) for two pairs of theoretical model cross sections. The black curves correspond to the effective-range cross section Eq. (2) and the gray curves are numerically calculated for a model potential consisting of a Morse potential well at short range, smoothly joined to a van der Waals tail at long range. The full curves are calculations for a $(^{52}\text{Cr}) = 170 a_0$ obtained from the low

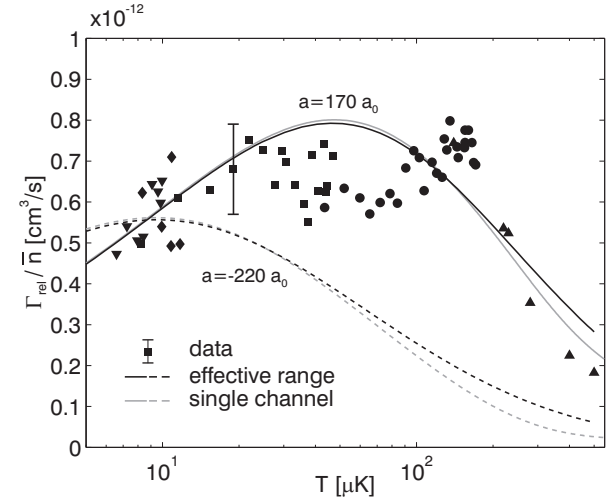


FIG. 3: Temperature dependence of the density-normalized rethermalization rate for ^{52}Cr . The black curves are obtained from Eq. 1 and 2, gray curves are single-channel calculations. Solid (dashed) curves correspond to a scattering length of $170 a_0$ ($-220 a_0$). The data have been compiled from five runs under different experimental conditions which are represented by different symbols.

temperature fit in Fig. 2, whereas we have assumed a negative scattering length $a = -220 a_0$ and the corresponding effective range $r_e = 229 a_0$ for the dotted curves. The latter combination of values has been chosen to achieve the best agreement with the relaxation data at low temperatures under the condition that a be negative. Fig. 3 shows the main results of the paper: (i) The comparison between the experimental data and the theoretical curves clearly shows that the assumption of a negative scattering length is incompatible with the relaxation data. (ii) The effective-range cross section agrees very well with the single-channel calculations over the measured temperature range. The small deviation of the relaxation rates from the theoretical curves with $170 a_0$ in the intermediate temperature range deserves further investigation.

Knowledge of the scattering lengths for two different isotopes of the same atomic species can give further insight into the molecular potentials involved in the collision. We have therefore performed additional relaxation measurements on ^{50}Cr , which is also a boson with vanishing nuclear spin. In Fig. 4 we have plotted the results for the density-normalized relaxation rates for ^{50}Cr (black circles). For comparison, we have included again the data for ^{52}Cr (gray squares) demonstrating that the relaxation rates for ^{50}Cr are much smaller than those for ^{52}Cr . All curves are obtained from the numerical single-channel calculation. The black solid curve is a fit to the ^{50}Cr data resulting in a scattering length of $a(^{50}\text{Cr}) = (40 \pm 15) a_0$, where we have again assumed a systematic uncertainty on the order of 20%. For the dashed curve we have as-

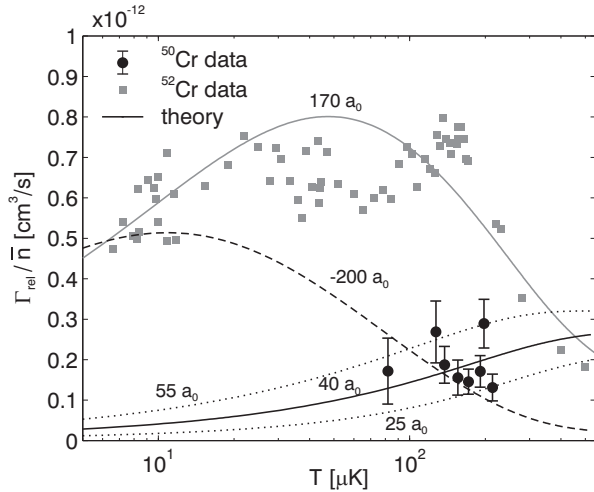


FIG. 4: Comparison of relaxation rates for ^{50}Cr (black circles) and ^{52}Cr (gray squares) normalized to the density. The black solid curve is a fit of the single-channel numerical calculation described in the text to the ^{50}Cr data yielding $a(^{50}\text{Cr}) = (40 \pm 15) a_0$. All other curves are the result of single-channel calculations with the indicated scattering lengths.

sumed a negative scattering length, where $a = -200 a_0$ gave the best agreement with the data. Mass scaling our scattering length from ^{52}Cr to ^{50}Cr for a variable number of deca-triplet bound states gives very strong evidence for a positive sign for $a(^{50}\text{Cr})$.

Our analysis yields effective s-wave scattering lengths, since the rather strong magnetic dipole-dipole interactions in chromium (6 Bohr magnetons) have been neglected. However, preliminary multichannel calculations show that the influence of the spin-dipolar interaction should be within our error bars.

In conclusion, we have measured the temperature-dependence of the scattering cross section for ^{52}Cr and for ^{50}Cr in ultracold spin-polarized samples. We obtain for the deca-triplet scattering lengths $a(^{52}\text{Cr}) = (170 \pm 39) a_0$ and $a(^{50}\text{Cr}) = (40 \pm 15) a_0$. The positive sign of $a(^{52}\text{Cr})$ was deduced from a simple effective-range theory. This result together with model calculations provides strong evidence for a positive sign of $a(^{50}\text{Cr})$. In particular, the reasonably large value of $a(^{52}\text{Cr})$ and its sign make ^{52}Cr a promising candidate for achieving BEC.

Our findings supplement spectroscopic data on chromium dimers [25], which are only available for the singlet potential and should thus help improve the accuracy of theoretical calculations of molecular potentials [26] and of collision properties of chromium. Of particular interest would be the determination of the position and width of magnetically tunable Feshbach resonances. If Feshbach resonances are readily accessible, chromium with its large dipole moment would be an ideal system for studying the interplay between contact and dipolar

interaction since both interactions could then be experimentally controlled [27].

We wish to thank the NIST, Gaithersburg, Atomic Physics Division led by P. S. Julienne for the ground-state collisions code and F. P. Pirani for useful comments on the C_{12} potential. This work was funded by the Forschergruppe "Quantengase" of the DFG and the European RTN "Cold Quantum Gases" under Contract No. HPRN-CT-2000-00125. P.O.S has been supported by the Studienstiftung des deutschen Volkes.

Electronic address: p.schmidt@physik.uni-stuttgart.de

- [1] J. R. Anglin and W. Ketterle, *Nature* **416**, 211 (2002).
- [2] C. Bradley, C. Sackett, J. Tollett, and R. Hulet, *Phys. Rev. Lett.* **75**, 1687 (1995), *ibid.* **79**, 1170 (1997).
- [3] D. G. Fried, T. C. Killian, L. W.iland, D. Landhuis, S. C. Moss, D. K. Leppner, and T. J. Greytak, *Phys. Rev. Lett.* **81**, 3811 (1998).
- [4] S. Comish, N. Claussen, J. Roberts, E. Cornell, and C. Wieman, *Phys. Rev. Lett.* **85**, 1795 (2000).
- [5] T. Weber, J. Herbig, M. Mark, H.-C. Nagerl, and R. Grimm, *Science* **299**, 232 (2003).
- [6] K. Goral, K. Raczewski, and T. Pfau, *Phys. Rev. A* **61**, 051601(R) (2000).
- [7] J. Weiner, V. S. Bagnato, S. Zilio, and P. S. Julienne, *Rev. Mod. Phys.* **71**, 1 (1999).
- [8] D. Heinzen, in *Proceedings of the International School of Physics - Enrico Fermi*, edited by M. Inguscio, S. Stringari, and C. Wieman (IOS Press, 1999), p. 351.
- [9] C. Saelius, E. Tiesinga, T. Laue, M. Eibl, H. Knoekel, and E. Tiesinga, *Phys. Rev. A* **63**, 012710 (2001).
- [10] C. Chin, V. Vuletic, A. J. Kerman, and S. Chu, *Phys. Rev. Lett.* **85**, 2717 (2000).
- [11] P. J. Leo, C. J. Williams, and P. S. Julienne, *Phys. Rev. Lett.* **85**, 2721 (2000).
- [12] A. Marte, T. Volz, J. Schuster, S. Durr, G. Rempe, E. G. M. van Kempen, and B. J. Verhaar, *Phys. Rev. Lett.* **89**, 283202 (2002).
- [13] C. Monroe, E. Cornell, C. Sackett, C. Myatt, and C. Wieman, *Phys. Rev. Lett.* **70**, 414 (1993).
- [14] G. Ferrari, M. Inguscio, W. Jastrzebski, G. Modugno, G. Roati, and A. Simoni, *Phys. Rev. Lett.* **89**, 053202 (2002).
- [15] P. O. Schmidt, S. Hensler, J. Wemer, T. Binhammer, A. Gorlitz, and T. Pfau, *J. Opt. B: Quantum Semiclass. Opt.* **5** (2003), in press, quant-ph/0211032.
- [16] P. O. Schmidt, S. Hensler, J. Wemer, T. Binhammer, A. Gorlitz, and T. Pfau, *J. Opt. Soc. Am. B* **20** (2003), in press, quant-ph/0208129.
- [17] S. A. Hopkins, S. Webster, J. Arlt, P. Bance, S. Comish, O. Matago, and C. J. Foot, *Phys. Rev. A* **61**, 032707 (2000).
- [18] M. Andert, M. B. Dahan, D. Guery-Odelin, M. Reynolds, and J. Dalibard, *Phys. Rev. Lett.* **79**, 625 (1997).
- [19] G. Kavoulakis, C. Pethick, and H. Smith, *Phys. Rev. A* **61**, 053603 (2000).
- [20] C. Joachain, *Quantum collision theory* (North-Holland publishing company, Amsterdam, 1975).
- [21] B. Gao, *Phys. Rev. A* **58**, 4222 (1998).

- [22] V. V. Flambaum, G. F. Grubakin, and C. Harabati, Phys. Rev. A 59, 1998 (1999).
- [23] R. Cambi, D. Cappelletti, G. Liuti, and F. Pirani, J. Chem. Phys. 95, 1852 (1991).
- [24] P. S. Julienne and F. H. Mies, J. Opt. Soc. Am. B 6, 2257 (1989).
- [25] S. M. Casey and D. G. Leopold, J. Phys. Chem. 97, 816 (1993).
- [26] K. Andersson, Chem. Phys. Lett. 237, 212 (1995).
- [27] S. G. Iovanazzi, A. G. Orlitz, and T. P. Fau, Phys. Rev. Lett. 89, 130401 (2002).
- [28] The factor = 2.65 has been obtained from [19], Eq. (88).